1

Human Papillomavirus Type 16 L1/L2 VLP Experimental Internalisation by Human

Peripheral Blood Leukocytes

Running Title: HPV16 VLP internalisation in human leukocytes.

Aurora Marques Cianciarullo[1,2#], Vivian Szulczewski[1,2], Erica Akemi Kavati[1,2], Tania

Matiko Hosoda[1,2], Elizabeth Leão[4], Primavera Borelli[5], Enrique Boccardo[6], Martin Müller[7],

Balasubramanyam Karanam[8], and Willy Beçak[1,9]

[1]Laboratory of Genetics, Butantan Institute, Secretary of State for Health, 1500 Dr Vital

Brazil Avenue, Sao Paulo, SP 05503-900, Brazil.

[2]Program of Postgraduate Interunits in Biotechnology USP-IBU-IPT, Institute of

Biomedical Sciences, University of Sao Paulo, 2415 Prof Lineu Prestes Avenue,

Biomedical III Building, University City, Sao Paulo, SP 05508-900, Brazil.

[3]Program of Professional Upgrading at Butantan Institute, Secretary of State for Health,

188 Dr Eneas de Carvalho Aguiar, Sao Paulo, SP 05403-000, Brazil.

[4]ELSME – Dr Elizabeth Leão Specialised Medical Services S/C Ltd., Sao Joaquim

Hospital, Real and Meritorious Portuguese Beneficence Association, 694 Martiniano de

Carvalho Street, Sao Paulo, SP 01321-000, Brazil.

25   [5]Laboratory of Experimental and Clinical Haematology, Department of Clinical and

26   Toxicological Analyses, School of Pharmaceutical Sciences, University of Sao Paulo, 580

27   B17 Prof Lineu Prestes Avenue, University City, Sao Paulo, SP 05508-900, Brazil.

28

29   [6]Laboratory of Oncovirology, Department of Microbiology, Institute of Biomedical

30   Sciences, University of Sao Paulo, 1374 Prof Lineu Prestes Avenue, Biomedical II

31   Building, University City, Sao Paulo, SP 05508-900, Brazil.

32

33   [7]Tumorvirus-specific Vaccination Strategies, Infection, Inflammation and Cancer Program,

34   German Cancer Research Centre (DKFZ), 242 Im Neuenheimer Feld, Heidelberg 69120,

35   Germany.

36

37   [8]Department of Pathology, Johns Hopkins University, Room 38, Cancer Research Building

38   2, 1550 Orleans Street, Baltimore, MD 21231, USA.

39

40   [9]Department of Biology, Federal University of the Latin-America Integration – UNILA,

41   1842 Silvio Americo Sasdelli Avenue, Vila A, Commercial Lorivo Building, Foz do

42   Iguaçu, PR 85866-000, Brazil.

43

44   **#Corresponding author:** Aurora M. Cianciarullo, Laboratory of Genetics, Butantan

45   Institute, 1500 Dr Vital Brazil Avenue, Sao Paulo, SP 05503-900, Brazil, phone +5511

46   26279725, fax +5511 26279714, email: aurora.cianciarullo@butantan.gov.br

47

48 **Footnote:** B.K. present addresses Department of Biology and Cancer Research, 1200 W.

49 Montgomery Road, Tuskegee University, Tuskegee, AL 36088, USA.

50

51 **Keywords:** HPV16 L1/L2 VLP, HPV internalisation by lymphocytes, HPV membrane

52 receptors, cancer risk factor, public health.

53

57

58 **Conflicts of interest:** The authors disclose no potential conflict of interest with the

59 publication of this article.

60

61 **Authors email:** aurora.cianciarullo@butantan.gov.br, emefjmlisboa@prefeitura.sp.gov.br,

62 erica.kavati@butantan.gov.br, hosodatania@yahoo.com.br, eleao@ibest.com.br,

63 borelli@usp.br, eboccardo@usp.br, martin.mueller@dkfz.de,

64 bkaranam@mytu.tuskegee.edu, wbecak@yahoo.com

65

66

67

68

69

70

71

ABSTRACT

Human papillomavirus (HPV) accounts for hundreds of thousands of new cases of cervical cancer yearly, and half of these women die of this neoplasia. This study investigates the possibility of HPV16 to infect human peripheral blood leukocytes in *ex vivo* assays. We have developed a leukocyte separation method from heparinized blood samples aiming cellular integrity and viability. We have expressed humanized L1 and L2 viral capsid proteins in HEK293T epithelial human cells, transiently transfecting them with vectors encoding humanized HPVL1 and L2 genes. Recombinant L1/L2 capsid proteins and structured virus-like particles interacted with human peripheral blood mononuclear cells – lymphocytes and monocytes – and were internalised through a pathway involving CD71 transferrin receptors. This was observed, at a percentile of about 54% T-CD4, 47% T-CD8, 48% B-CD20, and 23% for monocytes-CD14. The group of polymorph nuclear cells: neutrophils-eosinophils-basophils group did not internalise any VLPs. Blockage assays with biochemical inhibitors of distinct pathways, like chlorpromazine, rCTB, filipin, nystatin, liquemin, and sodium azide also evidentiated the occurrence of virus-like particles' indiscriminate entrance via membrane receptor on mononuclear cells. This study shows that HPV16 L1/L2 VLPs can interact with the plasma membrane surface and successfully enter lymphocytes without requiring a specific receptor.

IMPORTANCE

Human papillomaviruses (HPVs) belong to the *Papillomaviridae* family and are classified in Alpha papillomavirus, Beta papillomavirus, Gamma papillomavirus, and Mu papillomavirus genera, based on DNA sequence of the L1 gene. They are associated with the development of benignant skin warts, cell transformation and malignant tumours. L1 is

4

96   its major capsid protein, and L2 is the minor HPV capsid protein. HPV type 16 is

97   considered a high-risk Alpha papillomavirus due to the association with 50% of cervical

98   cancers worldwide. The most frequent HPV-associated cancer type is cervical cancer, but

99   etiological association has also been demonstrated for carcinomas of the penis, vulva,

100   vagina, anus and oropharynx – including base of the tongue and tonsils – regions. This

101   study indirectly investigates the possibility of HPV16 to infect other cell types *in vitro*,

102   particularly human peripheral blood leukocytes.

103

104   **INTRODUCTION**

105   In 1974, zur Hausen's researches pointed to the HPV as the major aetiological agent in

106   cervical cancer and, later, its DNA was detected in tumours found in other anogenital

107   regions (1-3). Today, there are more than 200 different types of well characterized HPVs,

108   of which approximately 40 types infect the genital tract. The most frequently found are

109   types 6 and 11 that induce benignant skin warts formation, and types 16 and 18 which are

110   associated to cancer development. There are at least 12 HPV types that according to the

111   Agency for Research on Cancer (IARC) are considered oncogenic to humans (4,

112   Papillomavirus Episteme (PaVE); http://pave.niaid.nih.gov/#home). Among them, HPV16

113   and HPV18 are those responsible for approximately 70% of all cervical cancers (4, 5). In

114   2025, the projected global estimate of cervical cancer is expected to rise to 720,415 new

115   cases per year, and it is expected that half of these women will die of this neoplasia (5).

116   However, the difficulty to obtain enough viable wild types or recombinant HPV particles

117   has limited researches to distinct aspects of virus biology (6). All viruses enter host cells to

118   survive, replicate and evade the immune system. So far, the entry of HPV and its traffic

119   through the host cells are still not completely elucidate (7). Several studies describe this

5

120   process like a complex set of interactions among different pathways, receptors, co-receptors

121   and co-factors. In keratinocytes, HPV seems to be internalised via clathrin-dependent

122   endocytic mechanisms, but it might use alternative uptake pathways to enter cells, such as a

123   caveolae-dependent route, among others depending on viral type (6-9).

124   Currently, HPV is recognised as one of the main causes of infection-related cancer

125   worldwide, as well as the causal factor of other diseases. Infection with high-risk HPV

126   types is the aetiological cause of cervical cancer and is strongly associated with a

127   significate fraction of penile, vulvar, vaginal, anal and oropharyngeal cancers (10, 11).

128   HPVs are responsible for approximately 88% of anal cancer and 95% of anal intraepithelial

129   neoplasia grades 2/3 lesions, and 40%-50% of penis and vulvar cancers (10). In

130   oropharyngeal cancers, HPV DNA was detected in 35%-50% cases (10). In all HPV-

131   positive non-cervical cancers, HPV16 is the most common HPV type detected, followed by

132   HPV types 18, 31, 33 and 45. Among the non-cancerous HPV-associated conditions,

133   genital warts and recurrent respiratory papillomatosis are surely linked to HPV6 and 11

134   (10). In addition, it was demonstrated recently that HPV16 virus-like particles (VLPs)

135   L1/L2 interact with haematopoietic precursor stem cells, present in the amniotic fluid from

136   healthy pregnant women (12). Whereas new pathologies are increasingly being associated

137   to the HPVs; the responsibility and costs of HPV-associated diseases and cancer remain an

138   important public health issue in all countries, regardless of their economic developmental

139   level (13). Due to the continuous worldwide propagation of HPV it is necessary to

140   investigate the possibility of HPV internalisation by different human cell types. In the

141   present study, we addressed the capacity of HPV16 L1/L2 VLP entrance/uptake of – in

142   peripheral blood leukocytes *in vitro*.

143

6

144 **MATERIAL AND METHODS**

145 **Production of HPV16 L1/L2 VLPs**

146 The production of VLPs was carried out throughout the recombinant protein expression

147 HPV16 L1 and L2 in epithelial human cells of the HEK293T lineage, cultured as

148 previously described (14). Transfection of these cells occur in a transient way using

149 pUF3L1h and pUF3L2h vectors, which are regulated by the human cytomegalovirus

150 promoter containing complete sequences of genes L1 and L2 – a method already described

151 in detail (14, 15). In this study, besides being used to produce VLPs containing both capsid

152 proteins, HEK293T cell line was also used as a control factor on interaction assays with

153 human peripheral blood leukocytes. All assays performed in this study were analysed in

154 duplicate, being representative of at least four independent tests.

155

156 **Blood collection**

157 Blood samples from 10 healthy female volunteers, ages ranging from 35 to 55, were

158 requested based on epidemiological data associated with genital HPV infection (16). The

159 screening of the volunteers was based on recent blood, Pap smears and colposcopy tests

160 and on data filled out by the candidate on a written informed consent form and on a

161 questionnaire, for the purpose of laboratory research. Volunteers who did not present Pap

162 and colposcopy results within reference values were dismissed. Blood samples were

163 collected in sterile tubes containing heparin – for interaction assays with leukocytes – and

164 EDTA – for blocking assays – , and were processed quickly, within a maximum of 2-hours

165 after collection. During this interval, they were stored at 4^oC.

166

167 **Leukocytes' separation**

7

168 Whole blood was collected in heparin at a concentration of 0.1 mg/ml, centrifuged at 1,000

169 rpm for 7 minutes at 5°C in a Sorvall$^®$ RT 6000 Refrigerated Centrifuge (Du Pont,

170 Wilmington-DE, USA) with a horizontal angle rotor. The plasma supernatant containing

171 platelets and leukocytes was gently removed and transferred with the aid of a Pasteur

172 pipette to a new tube. An aliquot was collected for total and differential counts, performed

173 in a Neubauer chamber, diluted (ratio 1:1) in Trypan blue and smears were stained by May-

174 Grünwald-Giemsa in order to determine their composition. Leukocytes sedimented were

175 centrifuged again at 1,200 rpm, for 3 minutes, at 5°C, to remove platelets. Leukocytes

176 precipitates were resuspended in 0.85% saline solution for subsequent tests (17). The

177 Neubauer chamber counts and smears containing distinct cell types were analysed by light

178 microscopy, with a Leica DMIL I microscope (Leica Microsystems GmbH, Vienna, AUT).

179

180 **Interaction assays of HEK293T cells and HPV16 L1/L2 VLPs**

181 HEK293T cells (2x10^4 cells/ml) were plated and maintained under growth conditions,

182 washed with PBS and incubated with 120 µg of VLPs in DMEM without FBS, for 4-hours

183 at 37°C and 5% CO_2. After this, cells were washed twice with PBS for 3 minutes each in

184 order to remove non-interactive particles. Cells were then fixed with 2%PFA

185 (Paraformaldehyde, Sigma-Aldrich) in PBS for 1-hour, at 4°C, and washed three times with

186 PBS, 5 minutes each. Plates were kept at 4°C until immunofluorescence assays. Controls

187 were performed in the absence of VLPs and/or the denaturation thereof, by heating at

188 100°C for 10 minutes (18, adapted).

189

190 **Interaction assays of human leukocytes and HPV16 L1/L2 VLPs**

8

191   Leukocytes ($2x10^4$ cells/ml) of healthy volunteers were incubated with 120 µg of VLPs

192   produced in this study and RPMI without FBS for 4-hours at 37^oC and 5% CO_2, under

193   gentle agitation. Cells were centrifuged at 1,000 rpm for 7 minutes and cell pellets washed

194   three times with PBS, 5 minutes each. Then, cells were fixed with 2% PFA in PBS for 1-

195   hour, at 4^oC. After this step, the centrifugation and PBS washing processes were repeated.

196   Samples were kept at 4^oC until immunofluorescence assays. Controls were the same as

197   described above for HEK293T cells.

198

199   **Interaction assays of leukocytes, transferrin and HPV VLPs**

200   The same protocol described above was employed, with minor changes described below.

201   Leukocytes were incubated with 120 µg of VLPs in separate samples, as follows: the

202   HPV16 L1/L2 VLPs produced in this study, and L1 VLPs of HPV6, 11, 16 and 18 from

203   Gardasil® vaccine, used as control, kindly provided by Merck Sharp & Dohme. RPMI

204   without FBS, together with transferrin (Tf) conjugated to fluorochrome TexasRed®

205   (Molecular Probes™), were added (ratio 1:60, Tf:RPMI). Samples were kept for 15, 45, 60

206   and 120 minutes in an incubator at 37^oC and 5% CO_2, under gentle agitation. The other

207   procedures remained unchanged.

208

209   **Blocking assays for membrane receptors**

210   Leukocytes of healthy donors were counted and incubated in RPMI medium overnight over

211   coverslips containing poly-L-lysine (Sigma-Aldrich), at 37^oC and 5% CO_2. Then, cells

212   were washed and a fresh medium was placed together with specific biochemical inhibitors

213   of ligand uptake (Table 1), used isolated or associated, and incubated for 2 hours (18). After

214   incubation, cells were washed and 120 µg of HPV16 L1/L2 VLPs (19) were added and

215   incubated with medium for 4 hours. Cells were washed again and fixed in 2% PFA

216   solution. Immunofluorescence assays were carried out to detect the VLP-PBMC interaction

217   by confocal microscopy, using specific antibodies to recognise L1 and L2 proteins. Z-axis

218   3D images were obtained to confirm the presence of VLPs within cells.

219

220   **Immunofluorescence assays for internalisation analysis**

221   Leukocytes were washed and fixed as already described. Samples were incubated in PBS

222   containing 1% BSA for 5 minutes under gentle agitation. Later, cells were incubated with

223   the primary antibodies (suppl. Data – Table 1); diluted in PBS containing 0.01% Tween[®]

224   20 and 0.5% BSA – pH 8 – for 2 hours, under gentle agitation, at room temperature. They

225   were then washed three times with PBS for 10 minutes each, followed by incubation with

226   the corresponding secondary antibodies (suppl. Data – Table 2); conjugated with

227   fluorochromes; and diluted in PBS containing 0.01% Tween[®] 20 and 1.5% BSA for 1 hour,

228   under light stirring, at room temperature. Once more, they were washed three times with

229   PBS for 10 minutes each. Samples of leukocytes with transferrin and VLPs were labelled

230   with Phalloidin conjugated AlexaFluor[®] 594, incubated for 20 minutes. Immediately after

231   that, they were rinsed twice with PBS for 10 minutes each. Aliquots of cell suspension from

232   both items assayed were adhered over silanized slides, and mounted with 5 µl Mowiol[®] and

233   coverslips. Samples were kept at 4°C until CLSM analysis, using Confocal Laser Scanning

234   Microscope Zeiss 510 Meta of the Butantan Institute (FAPESP Process No. 2000/11624-5;

235   Carl Zeiss GmbH, Jena, DEU).

236

237   **RESULTS**

238   **Leukocytes' identification**

239   After isolation of leukocytes from healthy donors, control smears stained by May-

240   Grünwald-Giemsa method showed cell morphology preservation (17), presenting a positive

241   correlation with the control blood smears. Counts indicated approximately 98%

242   lymphocytes; 0.7% monocytes; 1.5% polymorph nuclear cells; 0.1% red blood cells and

243   0.1% platelets. The ultrastructure was well preserved for all cell types analysed, with well-

244   defined and intact membranes (17). The efficiency and speed of the method for obtaining

245   leukocytes, preserving morphology and cell viability was confirmed.

246

247   **Analysis of interaction between HEK293T cells and HPV16 L1/L2 VLPs**

248   HEK293T cells interaction with HPV16 L1/L2 VLPs was analysed by

249   immunofluorescence. We emphasize that the genome of this cell line does not contain any

250   HPV DNA sequences, but it contains Adenovirus DNA and SV40 T-Ag. After 4-hours at a

251   37°C interaction, cells were washed in order to remove any particles or proteins that did not

252   interacted with HEK293T cells. Then, cells were fixed and stained with the primary

253   antibody Camvir-1 (BD Biosciences – suppl. Data – Table 1) for L1 proteins and with L1

254   conformation-specific anti-VLP antiserum (Biodesign – suppl. data – Table 1). It was

255   therefore possible to observe the internalisation of VLPs in some cells. In these cells VLPs

256   were found in the cytoplasm, near the core region (suppl. data – Img. 1 A-D), stained with

257   anti-VLP. These results were confirmed by the overlap of images (suppl. data – Img. 1 A

258   and C), and by the most thoroughly detailed internalisation display on the Z-axis scanning

259   sections (suppl. data – Img. 1 B and D). The morphological evaluations show that probably

260   the VLPs' internalisation occurs simultaneously with a large number of particles, similar to

261   the formation of endocytic vesicle structures (suppl. data – Img. 1 C, white arrow). These

262   results suggest that after 4 hours, structured VLPs (suppl. data – Img. 1 A-D), as well as

263   non-structured VLPs – such as pentameric and monomeric forms of L1 stained with

264   Camvir-1 (suppl. data – Img. 1 E) – , were internalised in epithelial cells from the human

265   kidney (HEK293T), across the cell membrane (suppl. data – Img. 1 B and D). The negative

266   controls showed no immunostaining for L1 and VLPs and no changes in cell morphology

267   were detected (suppl. data – Img. 2).

268

269   **Analysis of interactions between human leukocytes and HPV16 L1/L2 VLPs**

270   L1/L2 particles were added to human leukocytes, for 4-hours at 37°C, and prepared for

271   indirect CLSM immunofluorescence analysis, in order to investigate the possibility of

272   interaction between the leukocytes and the HPV16 L1/L2 VLPs. Results indicate an

273   interaction of VLPs with peripheral blood mononuclear cells (PBMC) – T and B

274   lymphocytes and monocytes – from healthy women volunteers (Fig. 1). Structured HPV16

275   L1/L2 VLPs also interacted with and were internalised by leukocytes (Figs. 2 and 3). After

276   4-hours of interaction, in most leukocytes examined, these particles were found in the cell

277   cytoplasm, as was the case with HEK293T. These results were confirmed by the images'

278   overlap (Figs. 1 A, B and D; Figs. 2 and 3), and the detailed internalisation, as shown on

279   the Z-axis scanning sections (Fig. 2 C). Fig. 1 C (green arrow) shows VLPs across the cell

280   membrane. The Z-axis' sweep cuts were able to demonstrate the internalisation of the VLP

281   with a larger number of particles similar to the formation of endocytic vesicles structures

282   (Fig. 2 A, white arrow), like those found in HEK293T cells (suppl. data – Img. 1 C, white

283   arrow), a phenomenon endorsed by morphological evaluations. In Fig. 3, the interaction of

284   leukocytes with the VLPs is illustrated, showing the colocalisation of HPV16 L1/L2

285   proteins recognised by anti-L1 (green) and anti-L2 (red), respectively. This colocalisation

286   was expected in VLPs that are composed of these two proteins, as it might be seen from the

12

287   images' overlap (Fig. 3). Fig. 3 B shows the internalisation of VLPs by leukocytes in a

288   significant amount when compared to other interactions. At least 15 fields were analysed

289   per experiment, containing from 4 to 10 cells per field. The presence of structures similar to

290   vacuoles can also be observed (Fig. 3 B, blue arrow). Control assays showed no

291   immunostaining, neither with the antibodies used to detect L1 and L2 separately, nor with

292   structured HPV16 L1/L2 VLPs (suppl. data – Img. 3).

293

294   **Identification of human PBMC interactions with VLPs**

295   These cells were treated with antibodies in order to recognise specific cell membrane

296   receptors for each type (suppl. data – Table 1), and analysed by indirect

297   immunofluorescence using CLSM to identify PBMC interactions with HPV16 VLPs, after

298   4-hours incubation at 37°C. HPV16 VLPs interacted with *ex vivo* PBMC (Figs. 4-6). These

299   results were confirmed by the images' overlap (Figs. 4 and 5) and displayed detailed

300   internalisation on the Z-axis sections (Fig. 6). T and B lymphocytes showed greater

301   competence to internalise VLPs, at around 47%-52% of cells (Table 2). Through

302   morphological assessments, T-lymphocytes that internalised VLPs and were recognised by

303   anti-CD8 showed endocytic vesicles-like structures (Fig. 4 B, white arrow). Only 23% of

304   monocytes that were identified by anti-CD14 antibody interacted with the VLPs (Table 2).

305

306   **Analysis of the colocalisation of VLPs and transferrin (Tf) in human PBMC**

307   After 15 minutes, no colocalisation between L1 VLPs and exogenous Tf was detected

308   (Fig.7). Moreover, it was possible to show the internalisation of VLPs during this period.

309   After 45 minutes, colocalisation of VLPs with exogenous Tf in the cytoplasm of human

310   PBMC (Fig. 8 and 9, yellow arrows), and also with the TfR or CD71, was observed (Fig. 9

311   A-B, yellow arrows) suggesting that the iron pathway may be used to HPV internalisation.

312   All results were confirmed by the images' overlap, respectively (Figs. 7-9).

313   We compared the kinetics of internalization of Tf and TfR (CD71) with the colocalisation

314   of HPV16 L1/L2 VLPs produced in this study and with control HPV6, 11, 16, 18 L1 VLPs

315   derived from the Gardasil® vaccine (Fig. 10). After only 15 minutes of interaction it was

316   possible to observe colocalisation of TfR and Tf (Fig. 10 A-B, purple arrows) with both

317   L1/L2 VLPs (Fig. 10 A) as well as with Gardasil L1 VLPs (Fig. 10 B). By means of

318   morphological analysis, we were able to demonstrate the colocalisation of both VLPs – L1

319   and L1/L2 – with Tf and TfR in the leukocytes' cytoplasm, after a 45-minutes interaction

320   period (Fig. 10 C-D, white arrows). This colocalisation among VLPs, Tf and TfR was

321   found in approximately 50% of analysed cells. Within 60 minutes of interaction, we

322   observed a feeble colocalisation between Tf and VLPs in about 30% of the cells (Fig. 10 E-

323   F, orange arrows). No colocalisation was observed in the tests after 120 minutes. The

324   colocalisation was evidentiated in detail by three-dimensional figures stacked in Z-axis

325   (Fig. 10). The negative controls showed no signs of L1 and VLPs. However, it was possible

326   to observe exogenous Tf internalisation (suppl. data – Img. 4). Comparative testing of

327   L1/L2 VLPs produced in this study and of control L1 VLPs from Gardasil® vaccine

328   showed no significant differences in the analysed results.

329

330   **Analysis of the blocking assays of PBMC membrane receptors**

331   After successful identification of VLPs within leukocytes and their colocalisation with Tf

332   and TfR, a variety of biochemical inhibitors, known to inhibit distinct cellular processes,

333   was used to demonstrate the involvement of these and other different pathways of VLPs

334   entry in PBMC.

14

335 Chlorpromazine inhibits clathrin-mediated endocytosis of various plasma membrane

336 proteins. Nystatin is a sterol-binding agent that disassembles caveolae in the membrane.

337 rCTB (Clostridium toxin B) acts by shortening the actin filaments' length, by inhibiting its

338 process *in vitro*. Liquemin is related with the VLPs obstruction of internalisation through

339 the HSPG (Heparan sulphate proteoglycans) pathway. Sodium azide is an ATPase

340 inhibitor, which blocks particle movement towards the cell body and leads to a diffuse

341 random movement.

342 The use of these different biochemical inhibitors was not sufficient to block the HPV16

343 L1/L2 VLPs entry in the PBMC (Figs. 11-12). Chlorpromazine – although known for

344 blocking the clathrin pathway through CD71 receptor of Tf – was not able to inhibit VLPs

345 entrance inside PBMC in a satisfactory manner. The same occurred when rCTB, Filipin and

346 Nystatin, Liquemin and Sodium azide were used to block actin-dependent cell processes,

347 the caveolae pathway, the HSPG pathway, and endocytic pathways, respectively, either

348 assayed separately or associated in an all-inhibitors cocktail. These results suggest that

349 PBMC makes use of multiple internalisation pathways to uptake HPV16 particles.

350

351 **DISCUSSION**

352 Differently of many Beta and Gamma papillomavirus, Alpha papillomaviruses developed

353 immune system evasion strategies from the host, causing persistent and visible papillomas,

354 which sometimes evolving to cancers (20). Some HPV types including 16, 18, 31, 33, 35,

355 39, 45, 51, 52, 56, 58 and 59 have been classified as human carcinogens by the IARC,

356 being responsible for at least 4% of all human malignancies (4, 21, Papillomavirus

357 Episteme (PaVE); http://pave.niaid.nih.gov/#home). Infection by high-risk HPV types is

358 the major factor for the development of cervical cancer, and HPV DNA is also found in

15

359   tumours affecting other anogenital regions. Besides, they are being correlated with an

360   increasing proportion of oropharyngeal squamous cells carcinomas, and occurrences

361   affecting mainly tonsil and base of tongue regions are currently being documented in

362   particular geographic areas (22). A study describes women who have never experienced

363   sexual intercourse as having genital lesions caused by HPV, showing that, in addition to

364   sexual transmission, could have other forms of infection such as fomites and skin contact,

365   and maternal-foetal vertical transmission is also being considered as a probable infection

366   pathway (23-27).

367   Cell-virus interaction is the initial step in viral infection. Often, virus adsorption occurs on

368   the plasma membrane of susceptible cells. In general, the most common solution is that the

369   pathogen's intracellular trafficking occurs through and existing entry mechanism, mediated

370   via clathrin, caveolin, macropinocytosis, among others, moving inside cells to reach the

371   location where viral replication occurs (28). Transcytosis is used to move antigens and

372   protective antibodies across epithelial barriers. Similar to what seems to occur with HIV

373   (29), the transcytosis of HPV through epithelial cells, crossing cellular barriers, should also

374   be dependent on trafficking to the endocytic recycling pathway. The productive life cycle

375   of HPV is directly linked to epithelial differentiation. It is believed that the papillomavirus

376   is capable of maintaining the expression of structural genes, under tight control of the

377   regulatory mechanisms of transcription and translation (30). The L1 capsid protein of HPV,

378   regardless of the presence or absence of L2, has the property of forming structures that

379   mimic morphologically authentic virions, VLPs, which are being used as replacements for

380   HPV infected cell culture *in vitro* (8, 14, 31, 32). However, the presence of L2 seems to

381   confer greater stability to the virus and VLP, therefore, the viral capsid indeed seems to

382   contribute to the virus' infectivity (33). Most experimental models explore the process of

383   host cell interaction by molecular or biochemical methods, using cell lines from different

384   tissues and species in interactions with HPV L1 VLPs in their studies.

385   In the present work, we produced HPV L1/L2 VLPs (14, 15) to investigate the possibility

386   that these particles interact with human leukocytes, in order to understand possible

387   mechanisms involved in these interactions. We have developed a method for the isolation

388   of these cells (17), used in suspension at 37°C, thereby creating an *ex vivo* system as closely

389   as possible to the natural conditions of HPV16 infection, thus conceiving a novel

390   experimental model.

391   HPV16 recombinant proteins L1, L2 and VLPs were visualized in the perinuclear region of

392   HEK293T cells, in compliance with data described in the literature (34). The presence of

393   BPV (bovine papillomavirus) in lymphocytes has been discussed (35, 36). Using PCR

394   technique (Polymerase Chain Reaction) in samples taken from humans with anogenital

395   lesions, the presence of HPV16 in peripheral blood samples (37) and in plasma cells (38)

396   was detected. Besides, DNA of other HPV types has been found in PBMC (39, 40). The

397   presence of HPV in lymphocytes of patients treated for anogenital cancers suggests that the

398   virus can remain in these cells even after treatment. However, there are no convincing

399   evidences that support that lymphocytes carry/produce infectious HPV viral particles.

400   Nonetheless, the presence of HPV macromolecules in lymphocytes may play a role in viral

401   immune response.

402   The scientific literature discloses that papillomavirus exhibits specific tropism for species

403   and tissues. However, BPV1 particles, isolated from bovine warts, and HPV16 VLPs

404   interacted successfully with 14 cell lines derived from different species and tissues, as

405   demonstrated in two different studies (32, 41). Using our model to investigate this, HPV16

406   L1/L2 VLPs interacted *in vitro* and *ex vivo* with two very distinct human cells, epithelial

17

407 kidney cells and PBMC, respectively. After 4 hours of interaction, these particles'

408 internalisation occurred, showing a very similar distribution pattern on both cell types. In

409 both, L1 VLPs were located in the cytoplasm near the nucleus, suggesting that tissue

410 differences do not affect the ability of HPV16 VLPs to entry in different cell types, and that

411 pentameric and monomeric forms of L1 may also be internalised. The interaction between

412 VLPs and monocytes observed in this study showed colocalisation with CD14. As

413 macrophage precursors, apparently these cells are able to internalise particles at a much

414 larger amount if compared with lymphocytes. The unexpected colocalisation of CD14

415 membrane receptor and VLPs, as well as the morphological changes observed, suggest that

416 monocytes respond to this interaction as immune cells, in order to eliminate invading

417 microorganisms. CD14 is a 53-kDa molecule, expressed mainly in monocytes,

418 macrophages and granulocytes. It is also found as soluble protein in the serum (42). One

419 known function of this receptor is to bind the complex of LPS (bacterial

420 lipopolysaccharide). Macrophages expressing CD14 can respond to very small amounts of

421 LPS, and this interaction is required for activation of these cells (43). Some studies suggest

422 that the receptor CD16 (FcγRIII), present on the plasma membrane surface of neutrophils,

423 can bind to VLPs at mice splenocytes' surface, indicating that this receptor has a role to

424 play in immune response against viral capsid proteins (43, 44). It is necessary to clarify the

425 actual mechanisms involved in the interactions between CD14, CD16 and VLPs, in order to

426 better understand how the immune system can properly eliminate the HPV from the host.

427 Tf is a beta globulin responsible for the transport of iron (Fe), through plasma, to the

428 interior of cells. Besides hepatocytes, other cells in the body are able to synthesize it. The

429 TfR is a membrane protein expressed primarily in T and B lymphocytes, macrophages, and

430 proliferating cells such as homodimers with N-terminal cytoplasmic tails (42). TfR is

18

431   constantly being endocytosed by plasma membrane through clathrin-mediated endocytosis,

432   with the purpose of carrying ferric iron bound to Tf to the inside of cells. This Tf-TfR

433   complex is delivered to the early endosome into a lower pH medium, where iron is released

434   and TfR is recycled to the cell's surface (45). When evaluating the interactions between

435   HPV16 L1/L2 VLPs, HPV6, 11, 16, 18 L1 VLPs (Gardasil® vaccine) and unstructured

436   HPV16 L1 in PBMCs and in the presence of exogenous Tf, we determined the

437   colocalisation of L1-VLP-Tf and free Tf in these cells, as well as colocalisation with TfR,

438   after 45 minutes of interaction. This colocalisation between VLP, Tf and TfR was found in

439   approximately 50% of analysed cells. These results suggest that HPV16 L1/L2 VLPs,

440   HPV6, 11, 16, 18 L1 VLPs (Gardasil® vaccine) and unstructured HPV16 L1 can enter cells

441   by endocytosis through clathrin-dependent, via TfR. It is probable that, along viral infection

442   processes, interactions between HPV16 (about 55 nm size) and Tf molecules (80-kDa)

443   might indeed happen, through fusion with Fe-Tf-TfR complexes, mimicking its entry into

444   the cell via low pH endosomes, thus enabling transcytosis (29, 46-49).

445   There have been no reports in the literature showing the internalisation of HPV VLPs in

446   human PBMC. So far, this study has showed that PBMCs of healthy female volunteers

447   were able to internalise HPV16 VLPs. Also, T and B Lymphocytes were the main cell

448   types that further interacted with VLPs. It is important to emphasize that the lymphocytes

449   are cells capable of dividing themselves and it is estimated that the half-life of these

450   inactive cells in humans is of some years. Furthermore, inactive lymphocytes circulate

451   continuously through the bloodstream and lymphatic vessels. Using different cell lineages

452   with VLPs or PsV (pseudovirion), scientists have come to different conclusions. Our

453   findings agree with the data obtained by other researchers who – through the use of PsV-

454   infected HeLa and HaCaT cells – successfully demonstrated that the HPV entry is clathrin-

19

455 caveolin-cholesterol-and-dynamin-independent (7). The entry of HPV VLPs in leukocytes

456 by independent endocytosis pathways may be due to their ability to recognise, capture and

457 remove foreign substances from the body. The use of different biochemical inhibitors,

458 isolated or associated, does not seem to be enough to block the internalisation of HPV16

459 L1/L2 VLPs in the PBMC, suggesting that a specific receptor is not required to the uptake

460 and HPV16 entry into the host cells. A recent study demonstrates that intrinsic risk factors

461 are responsible of around 10%-30% of cancer development risk, and that the rates of

462 endogenous mutation accumulation by intrinsic processes are not sufficient to account for

463 the high cancer risks observed. Cancer risk in general is heavily influenced by extrinsic

464 factors like HPV infection (50). Unravelling the molecular steps leading to virus entry into

465 the cells may be important for the development of new strategies for the prevention of

466 infection by HPV and foster immune response against important human pathogen.

467

468 **CONCLUSIONS**

469 HPV16 L1/L2 VLPs produced in this study interacted with *in vitro* HEK293T cells and *ex*

470 *vivo* PBMC from healthy women volunteers, and were internalised. This study evinced that

471 HPV16 L1/L2 VLPs can interact with the plasma membrane surface, and been uptake by

472 lymphocytes. We also demonstrated that HPV16 L1/L2 VLPs might utilize the endocytic

473 pathway of iron-mediated clathrin as a receptor, which involves multiple membrane

474 receptors simultaneously and also the classical endocytic pathway of iron – the most

475 widespread among vertebrates and the animal kingdom as a whole – we have demonstrated

476 that HPV16 L1/L2 VLPs does not require a specific receptor in order to be internalised by

477 leukocytes. Complementary studies are required to accurately demonstrate the probable

478 mechanisms involved.

20

479

ACKNOWLEDGEMENTS

488

Ethical Committee

490 This work was duly evaluated and approved by the Sao Joaquim Hospital, Real and

491 Meritorious Portuguese Beneficence Association Ethical Committee on Human Research.

492 Protocol number: 369-08.

493 This work is in full compliance with the National Biosafety Law (CTNBio) guidelines and

494 the present study was approved by the Butantan Institute Institutional Biosafety Committee

495 (CIBio) and CTNBio – Process Nr. 01200.004893/1997-93 – published in the Brazilian

496 Official Gazette (DOU) on August 16, 2011.

497

REFERENCES

499 1. **zur Hausen H, Meinhof W, Scheiber W, Bornkamm GW.** 1974. Attempts to

500 detect virus-specific DNA sequences in human tumors: I. Nucleic acid

501 hybridizations with complementary RNA of human wart virus. Int J Cancer **13:**650-

502   656. (First negative attempt to find papillomavirus DNA in cancer of the cervix with

503   labelled HPV DNA from plantar warts).

504   2. **zur Hausen H.** 1976. Condylomata acuminata and human genital cancer. Cancer

505   Res **36:**794. (Hypothesis that papillomaviruses are involved in the etiology of cancer

506   of cervix).

507   3. **Dürst M, Dzarlieva-Petruseyska RT, Boukamp P, Fusenig NE, Gissmann L.**

508   1987. Molecular and cytogenetic analysis of immortalized human primary

509   keratinocytes obtained after transfection with human papillomavirus type 16 DNA.

510   Oncogene **1:**251-256.

511   4. **Viarisio D, Gissmann L, Tommasino M.** 2017. Human papillomaviruses and

512   carcinogenesis: well-established and novel models. Curr Opin Virol **26:**56-62.

513   5. **Sanjosé S, Serrano B, Castellsagué X, Brotons M, Muñoz J, Bruni L, Bosch FX.**

514   2012. Human papillomavirus (HPV) and related cancers in the Global Alliance for

515   Vaccines and Immunization (GAVI) countries. AWHO/ICO HPV Information

516   Centre Report. Vaccine **30S:**D1-D83.

517   6. **Day PM, Lowy DR, Schiller JT.** 2003. Papillomaviruses infect cells via a clathrin-

518   dependent pathway. Virology **307:**1-11.

519   7. **Raff AB, Woodham AW, Raff LM, Skeate JG, Yan L, Da Silva DM, Schelhaas**

520   **M, Kast WM.** 2013.The evolving field of human papillomavirus receptor research:

521   a review of binding and entry. J Virol **87:**6062-6072.

522   8. **Bousarghin L, Touzé A, Combita-Rojas AL, Coursaget P.** 2003. Positively

523   charged sequences of human papillomavirus type 16 capsid proteins are sufficient to

524   mediate gene transfer into target cells via the heparan sulfate receptor. J Gen Virol

525   **84:**157-164.

526   9. **Hindmarsh PL, Laimins LA.** 2007. Mechanisms regulating expression of the HPV

527   31 L1 and L2 capsid proteins and pseudovirion entry. Virol J **4:**1-12.

528   10. **Bosch FX, Broker TR, Forman D, Moscicki AB, Gillison ML, Doorbar J, Stern**

529   **PL, Stanley M, Arbyn M, Poljak M, Cuzick J, Castle PE, Schiller JT,**

530   **Markowitz LE, Fisher WA, Canfell K, Denny LA, Franco EL, Steben M, Kane**

531   **MA, Schiffman M, Meijer CJ, Sankaranarayanan R, Castellsagué X, Kim JJ,**

532   **Brotons M, Alemany L, Albero G, Diaz M, Sanjosé S**. 2013. Authors of ICO

533   Monograph Comprehensive Control of HPV Infections and Related Diseases.

534   Vaccine **31:**H1-31. Collaborators (98)

535   11. **Alemany L, Saunier M, Alvarado I, Quirós B, Salmeron J, Shin HR, Pirog E,**

536   **Guimerà N, Hernández GA, Felix A, Clavero O, Lloveras B, Kasamatsu E,**

537   **Goodman MT, Hernandez BY, Laco J, Tinoco L, Geraets DT, Lynch CF,**

538   **Mandys V, Poljak M, Jach R, Verge J, Clavel C, Ndiaye C, Klaustermeier J,**

539   **Cubilla A, Castellsagué X, Bravo IG, Pawlita M, Quint W, Muñoz N, Bosch FX,**

540   **Sanjosé S on behalf of the HPV VVAP study group.** 2015. HPV DNA prevalence

541   and type distribution in anal carcinomas worldwide. Int J Cancer **136:**98-107.

542   12. **Kavati EA, Palumbo ACM, Andrade FB, Marigliani B, Sakauchi D, Leão E,**

543   **Armbruster-Moraes E, Müller M, Cianciarullo AM.** 2012. Interaction of

544   HPV16L1L2 VLP with stem cells CD34+/CD117+ of the human amniotic fluid. In:

545   Current microscopy contributions to advances in science and technology. Editor:

546   Antonio Méndez-Vilas. Publisher: Formatex Research Center, Badajoz, Spain.

547   Volume **5:**617-624. ISBN-13: 978-84-939843-5-9.

548   http://www.formatex.info/microscopy5/book/617-624.pdf

23

549   13. **Dunne EF, Markowitz LE, Saraiya M, Stokley S, Middleman A, Unger ER,**

550   **Williams A, Iskander J.** 2014. Centers for Disease Control and Prevention. CDC

551   Grand Rounds: Reducing the Burden of HPV-Associated Cancer and Disease.

552   MMWR **63:**69-72.

553   14. **Cianciarullo AM, Szulczewski V, Chaves AAM, Bazan SB, Aires KA, Müller M,**

554   **Armbruster-Moraes E.** 2010. Production of HPV16 L1L2 VLPs in cultures of

555   human epithelial cells. In: Microscopy: Science, Technology, Applications and

556   Education. Editors: Antonio Méndez-Vilas and Jesús Díaz Álvarez. Publisher:

557   Formatex Research Center, Badajoz, Spain. Volume **4:**1073-1082. ISBN- 13: 978-

558   84-614-6190. http://www.formatex.info/microscopy4/ 1073-1082.pdf

559   15. **Marigliani B, Kavati EA, Sakauchi D, Oliveira HB, Canali RA, Sasaki AA,**

560   **Ferreira Jr JMC, Armbruster-Moraes E, Müller M, Cianciarullo AM.** 2012.

561   Intracellular distribution of recombinant Human Papillomavirus capsid proteins. In:

562   Current microscopy contributions to advances in science and technology. Editor:

563   Antonio Méndez-Vilas. Publisher: Formatex Research Center, Badajoz, Spain.

564   Volume **5:**678-684. ISBN-13: 978-84-939843-5-9.

565   http://www.formatex.info/microscopy5/book/678-684.pdf

566   16. **Nonnenmacher B, Breitenbach V, Villa LL, Prolla JC, Bozzetti MC.** 2002.

567   Genital human papillomavirus infection identification by molecular biology among

568   asymptomatic women. Rev Saude Publica **36:**95-100.

569   17. **Kavati EA, Hosoda TM, Szulczewski V, Leão E, Borelli P, Cianciarullo AM.**

570   2017. A simple, fast, inexpensive and efficient method for leukocytes separation

571   with preservation of morphology and cell viability for use in education and research.

572   In: Microscopy and imaging science: practical approaches to applied research and

573   education. Editor: Antonio Méndez-Vilas. Publisher: Formatex Research Center,

574   Badajoz, Spain. Volume **7:**665-670. ISBN-13: 978-84-942134-9-6.

575   http://www.microscopy7.org/book/665-670.pdf

576   18. **Fothergill T, Mcmillan NAJ.** 2006. Papillomavirus virus-like particles activate the

577   PI3-kinase pathway via alpha-6 beta-4 integrin upon binding. J Virol **352:**319-328.

578   19. **Van Hamme E, Dewerchin HL, Cornelissen E, Verhasselt B, Nauwynck HJ.**

579   2008. Clathrin- and caveolae-independent entry of feline infectious peritonitis virus

580   in monocytes depends on dynamin. J Gen Virol **89:**2147-2156.

581   20. **Doorbar J, Egawa N, Griffin H, Kranjec C, Murakami I.** 2015. Human

582   papillomavirus molecular biology and disease association. Rev Med Virol **25:**2-23.

583   21. **Schellenbacher C, Roden RBS, Kimbauer R.** 2017. Developments in L2-based

584   human papillomavirus (HPV) vaccines. Virus Res **231:**166-175.

585   22. **Näsman A, Nordfors C, Holzhauser S, Vlastos A, Tertipis N, Hammar U,**

586   **Hammarstedt-Nordenvall L, Marklund L, Munck-Wikland E, Ramqvist T,**

587   **Bottai M, Dalianis T.** 2015. Incidence of human papillomavirus positive tonsillar

588   and base of tongue carcinoma: a stabilisation of an epidemic of viral induced

589   carcinoma? Eur J Cancer **51:**55-61.

590   23. **Frega A, Cenci M, Stentella P, Cipriano L, De Ioris A, Alderisio M, Vecchione**

591   **A.** 2003. Human papillomavirus in virgins and behaviour at risk. Cancer Lett **194:**

592   21-24.

593   24. **Armbruster-Moraes E, Ioshimoto LM, Leão E, Zugaib M.** 1994. Presence of

594   human papillomavirus DNA in amniotic fluids of pregnant women with cervical

595   lesions. Gynecol Oncol **54:**152–158.

596   25. **Rombaldi RL, Serafini EP, Mandelli J, Zimmermann E, Losquiavo KP.** 2008.

597   Transplacental transmission of human papillomavirus. Virol J **5:**106.

598   26. **Sarkola ME, Grénman SE, Rintala MA, Syrjänen KJ, Syrjänen SM.** 2008.

599   Human papillomavirus in the placenta and umbilical cord blood. Acta Obstet

600   Gynecol Scand **87:**1181-1188.

601   27. **Koskimaa HM, Waterboer T, Pawlita M, Grénman S, Syrjänen K, Syrjänen S.**

602   2012. Human papillomavirus genotypes present in the oral mucosa of newborns and

603   their concordance with maternal cervical human papillomavirus genotypes. J Pediatr

604   **160:**837-843.

605   28. **Gruenberg J, van der Goot FG.** 2006. Mechanisms of pathogen entry through the

606   endosomal compartments. Nat Rev Mol Cell Biol **7:**495-504.

607   29. **Kinlock BL, Wang Y, Turner TM, Wang C, Liu B.** 2014. Transcytosis of HIV-1

608   through vaginal epithelial cells is dependent on trafficking to the endocytic recycling

609   pathway. PLoS ONE **9:**e96760.

610   30. **Müller M.** 2005. Human Papilloma Viruses: Methods and Protocols. Humana Press

611   Inc. In: Davy, C.; Doorbar, J. Methods in Molecular Medicine. Totowa, NJ.

612   **119:**435-446.

613   31. **Müller M, Gissmann L, Cristiano RJ, Sun XY, Frazer IH, Jenson AB, Alonso**

614   **A, Zentgraf H, Zhou J.** 1995. Papillomavirus capsid binding and uptake by cells

615   from different tissues and species. J Virol **69:**948-954.

616   32. **Roden RB, Kirnbauer R, Jenson AB, Lowy DR, Schiller JT.** 1994a. Interaction

617   of papillomaviruses with the cell surface. J Virol **68:**7260-7266.

618   33. **Kieback E, Müller M.** 2006. Factors influencing subcellular localization of the

619   human papillomavirus L2 minor structural protein. Virology **345:**199-208.

620   34. **Leder C, Kleinschmidt JA, Wiethe C, Müller M.** 2001. Enhancement of Capsid

621   Gene Expression: Preparing the Human Papillomavirus Type 16 Major Structural

622   Gene L1. J Virol **75:**9201-9209.

623   35. **Campo MS, Jarrett WF, Barron R, O'Neil BW, Smith KT.** 1992. Association of

624   bovine papillomavirus type 2 and bracken fern with bladder cancer in cattle. Cancer

625   Res **52:**6898-6904.

626   36. **Stocco dos Santos RC, Lindsey CJ, Ferraz OP, Pinto JR, Mirandola RS, Benese**

627   **FJ, Birgel EH, Bragança-Pereira CA, Beçak W.** 1998. Bovine papillomavirus

628   transmission and chromosomal aberrations: an experimental model. J Gen Virol

629   **79:**2127-2135.

630   37. **Tseng CJ, Lin CY, Wang RL, Chen LJ, Chang YL, Hsieh TT, Pao CC.** 1992.

631   Possible transplacental transmission of human papillomaviruses. Am. J. Obstet

632   Gynecol **166:**35-40.

633   38. **Payne D, Tyring SK, Doherty MG, Daya D, Chan TS.** 1993. Detection of human

634   papillomavirus type 16 in plasma cells. Gynecol Oncol **48:**406-412.

635   39. **Pao CC, Lin SS, Lin CY, Maa JS, Lai CH, Hsieh TT.** 1991. Identification of

636   human papillomavirus DNA sequences in peripheral blood mononuclear cells. Am J

637   Clin Pathol **95:**540-546.

638   40. **Karas Z, Porebas E.** 1998. HPV sequences in blood of patients with condyloma

639   acuminata. J Invest Dermatol **110:**843-844.

640   41. **Roden RB, Weissinger EM, Henderson DW, Booy F, Kirnbauer R, Mushinski**

641   **JF, Lowy DR, Schiller JT.** 1994b. Neutralization of bovine papillomavirus by

642   antibodies to L1 and L2 capsid proteins. J Virol **68:**7570-7574.

27

643   42. **Abbas AK, Lichtman AH.** 2005. Cellular and Molecular Immunology. 5 ed.

644   Philadelphia: Elsevier, 580 p.

645   43. **Da Silva DM, Velders MP, Nieland JD, Schiller JT, Nickoloff BJ, Kast WM.**

646   2001. Physical interaction of human papillomavirus virus-like particles with immune

647   cells. Int Immunol **13:**633-641.

648   44. **Da Silva DM, Fausch SC, Verbeek JS, Kast WM.** 2007. Uptake of human

649   papillomavirus virus-like particles by dendritic cells is mediated by Fc gamma

650   receptors and contributes to acquisition of T cell immunity. J Immunol **178:**7587-97.

651   45. **Trowbridge IS, Omary MB.** 1981. Human cell surface glycoprotein related to cell

652   proliferation is the receptor for transferrin. Proc Natl Acad Sci USA **78:**3039–3043.

653   46. **Tuma PL, Hubbard AL.** 2003. Transcytosis: crossing cellular barriers. Physiol Rev

654   **83:**871-932.

655   47. **Kinlock BL, Wang Y, Turner TM, Wang C, Liu B.** 2014. Transcytosis of HIV-1

656   through vaginal epithelial cells is dependent on trafficking to the endocytic recycling

657   pathway. PLoS One **9:**e96760.

658   48. **Anderson DJ.** 2014. Modeling mucosal cell-associated HIV type 1 transmission in

659   vitro. J Infect Dis **210:**S648-S653.

660   49. **Sakajiri T, Yamamura T, Kikuchi T, Yajima H.** 2009. Computational structure

661   models of apo and diferric transferrin-transferrin receptor complexes. Protein J

662   **28:**407-414.

663   50. **Wu S, Powers S, Zhu W, Hannun YA.** 2016. Substantial contribution of extrinsic

664   risk factors to cancer development. Nature **529:**43-47.

665

666

667   **Figure Legends**

668   **Figure 1:** Interactions of human leukocytes with VLPs of HPV16, detected by indirect

669   immunofluorescence. The leukocyte cells were incubated with the VLPs for 4 h. Following

670   fixation, they were immunostained with anti-HPV16 L1 antibody and then stained with a

671   secondary antibody conjugated to FITC (green). In all assays, AlexaFluor® 594-conjugated

672   Phalloidin (red) detected the actin cytoskeleton. The internalisation of VLPs (green arrows)

673   is shown in image C, through the sweep cuts on the Z-axis (C) 9.50 µm thick sections and

674   each section to 1.60 µm. CLSM Zeiss LSM 510 Meta. Magnification: Objective C-

675   Apochromatic 63xs /1.4 oil. Bar = 5 µm.

676

677   **Figure 2:** Interactions of human leukocytes with VLPs of HPV16, detected by indirect

678   immunofluorescence. The leukocyte cells were incubated with the VLPs for 4 h. Following

679   fixation, they were immunostained with the conformational anti-HPV16 VLPs and stained

680   with a secondary antibody conjugated to FITC (green). AlexaFluor® 594-conjugated

681   Phalloidin (red) detected the actin cytoskeleton. The internalisation of VLPs (green arrows)

682   is shown in image C, through Z-axis sweep cuts (C) 7.80 µm thick sections and each

683   section to 1.30 µm. In (A) we see a structure similar to an endocytic vesicle (white arrow).

684   CLSM Zeiss LSM 510 Meta. Magnification: Objective C-Apochromatic 63xs /1.4 oil. Bar

685   = 5 µm.

686

687   **Figure 3:** Interactions of human leukocytes with VLPs of HPV16, detected by indirect

688   immunofluorescence. After fixation, cells were immunostained with anti-HPV16 L1

689   antibody and then stained with a secondary antibody conjugated to FITC (green). Then

690   immunostained with anti-HPV16 L2 antibody and revealed by AlexaFluor®555 secondary

691   antibody (red). The internalisation of VLPs (yellow arrows) is shown in confocal images

692   (merge). In (B) structures similar to vacuoles (blue arrow) might be observed. CLSM Zeiss

693   LSM 510 Meta. Magnification: Objective C-Apochromatic 63xs /1.4 oil. Bar = 5 μm.

694

695   **Figure 4:** Identification of human leukocyte interactions with the HPV16 VLPs analysed

696   by indirect immunofluorescence. After fixation, cells were immunostained with the

697   conformational anti-HPV16 VLPs and revealed by a secondary antibody conjugated to

698   FITC (green). Then, the cells were treated with anti-CD04 (A) and anti-CD08 (B) and

699   stained with a secondary antibody AlexaFluor[®]546 (red). VLP internalisation (green

700   arrows) is visible on image overlay (merged images). In (B), a structure similar to an

701   endocytic vesicle is detectable (white arrow). CLSM Zeiss LSM 510 Meta. Magnification:

702   Objective C-Apochromatic 63xs /1.4 oil. Bar = 5 μm.

703

704   **Figure 5:** Identification of human leukocyte interactions with the HPV16 VLPs, analysed

705   by indirect immunofluorescence. After fixation, cells were immunostained with the

706   conformational anti-HPV16 VLPs and revealed by a secondary antibody conjugated to

707   FITC (green). Then, the cells were treated with anti-CD20 and anti-CD14 and stained with

708   a secondary antibody AlexaFluor[®]546 (red). VLP internalisation (green arrows) is visible

709   on image overlay (merged images). In (B) we can observe the colocalisation of CD14 and

710   VLPs (orange arrow) and vacuole-like structures (blue arrow). CLSM Zeiss LSM 510

711   Meta. Magnification: Objective C-Apochromatic 63xs /1.4 oil. Bar = 5 μm.

712

713   **Figure 6:** Identification of human leukocyte interactions with the HPV16 VLPs analysed

714   by indirect immunofluorescence. After fixation, cells were immunostained with the

715   conformational anti-HPV16 VLPs and revealed by a secondary antibody conjugated to

716   FITC (green). Then, the cells were treated with anti-CD20 (C), anti-CD04 (A), anti-CD08

717   (B), anti-CD14 (D) and AlexaFluor®546 revealed by secondary antibody (red). VLP

718   internalisation (green arrows) is shown in the images through Z-axis sweep cuts. (A) 9.25

719   μm of thick sections and each section of 0.84 μm; (B) 8.56 μm thick sections and each

720   section with 0.95 μm; (C) 9.27 μm thick sections and each section with 1.03 μm; (D) 10,94

721   μm thick sections and each section having 1.40 μm. CLSM Zeiss LSM 510 Meta.

722   Magnification: Objective C-Apochromatic 63xs /1.4 oil.

723

724   **Figure 7:** Colocalisation of VLPs of HPV16 and Tf in human leukocytes, detected by

725   indirect immunofluorescence. The leukocyte cells were incubated with the VLPs and the

726   conjugated Tf TexasRed® (red). Leukocytes were treated with anti-HPV16 L1 antibody,

727   revealed by a secondary antibody conjugated to FITC (green). In confocality (merge), the

728   images reveal colocalisation of L1 and Tf (yellow arrows). CLSM Zeiss LSM 510 Meta.

729   Magnification: Objective C-Apochromatic 63xs /1.4 oil. Bar = 5 μm.

730

731   **Figure 8:** Colocalisation of HPV16 VLPs and Tf in human white blood cells, detected by

732   indirect immunofluorescence. The leukocyte cells were incubated with the VLPs and the

733   conjugated Tf TexasRed® (red). Leukocytes were immunostained with anti-HPV16 VLP

734   antibody and revealed by a secondary antibody conjugated to FITC (green). In confocality

735   (merge), the images reveal colocalisation of VLPs and Tf (yellow arrows). CLSM Zeiss

736   LSM 510 Meta. Magnification: Objective C-Apochromatic 63xs /1.4 oil. Bar = 5 μm.

737

31

738   **Figure 9:** Three-dimensional imaging of leukocyte interactions with the VLPs produced in

739   this study or the VLP vaccine Gardasil, Tf and TfR; detected by indirect

740   immunofluorescence. The leukocyte cells were incubated with the VLPs and the conjugated

741   Tf TexasRed® (red). After fixation, the leukocytes were immunostained with anti-HPV16

742   VLP antibody and revealed by a secondary antibody, conjugated to FITC (green), then

743   treated with anti-CD71 and revealed by AlexaFluor®633 (blue). (A) and (B) colocalisation

744   Tf and TfR (purple arrow), (C) and (D) colocalisation VLP / Tf / TfR (white arrows), (E)

745   and (F) weak colocalisation VLP / Tf (orange arrows). CLSM Zeiss LSM 510 Meta.

746   Magnification: Objective C-Apochromatic 63xs /1.4 oil.

747

748   **Figure 10 (1-6):** Immunofluorescence assay detecting the HPV VLPs entry in PBMC, even

749   in presence of specific biochemical inhibitors of ligand uptake: (1) Sodium azide; (2)

750   Chlorpromazine; (3) Liquemin; (4) rCTB; (5) Filipin; (6) Nystatin. (a) shows the overlay

751   (merge) of images detected by stain of L1 protein (green), L2 protein (red), nuclei (blue);

752   (b) Z-axis showing L1 protein within cells; (c) Z-axis showing the entry of L2 protein in

753   cells was not inhibited. CLSM Zeiss LSM 510 Meta. Magnification: Objective C-

754   Apochromatic 63xs /1.4 oil. Bar = 5 μm.

755

756   **Figure 11.** Assay performed with all inhibitors used in Fig.15 (1-6), in association. (a)

757   Detection of L1 protein (green); (b) L2 protein within cells (red); (c) nuclei (blue); (d) the

758   overlay (merge) of images (a, b and c); Z-axis showing the L1 (e) and L2 (f) proteins within

759   cells. CLSM Zeiss LSM 510 Meta. Magnification: Objective C-Apochromatic 63xs /1.4 oil.

760   Bar = 5 μm.

761

Illustrations

Table 1: Biochemical inhibitors used to examine their effects on the entry of HPV VLPs in PBMC.

Inhibitors	Inhibition
Chlorpromazine	Clathrin pathway
rCTB (Clostridium toxin B)	Actin-dependent cells process
Filipin and Nystatin	Caveolae pathway
Liquemin	HSPG pathway
Sodium azide	Endocytic pathways

Table 2: Interactions of HPV16 VLPs produced in this study with PMBC (mononuclear cells) from peripheral blood of healthy female volunteers.
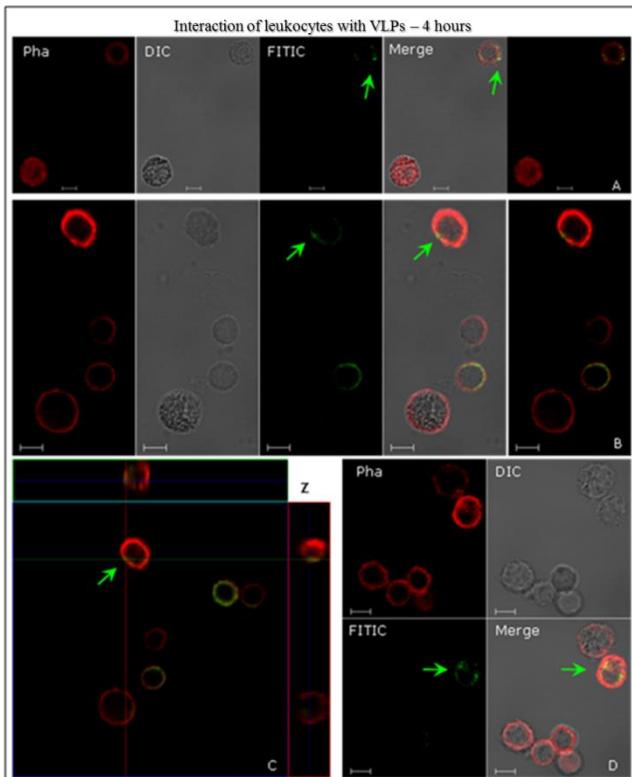
PMBC	Receptor	Percentage of cells that interacted with VLPs[1]
Lymphocyte T	CD04	52% ± 3
Lymphocyte T	CD08	47% ± 2
Lymphocyte B	CD20	48% ± 3
Monocyte	CD14	23% ± 5

[1] The percentage of cells that interact with HPV16 VLPs was calculated by the number of cells recognized by anti-CD antibodies, which have internalized the particles. The result corresponds to the analysis in duplicate, being representative of at least four trials.
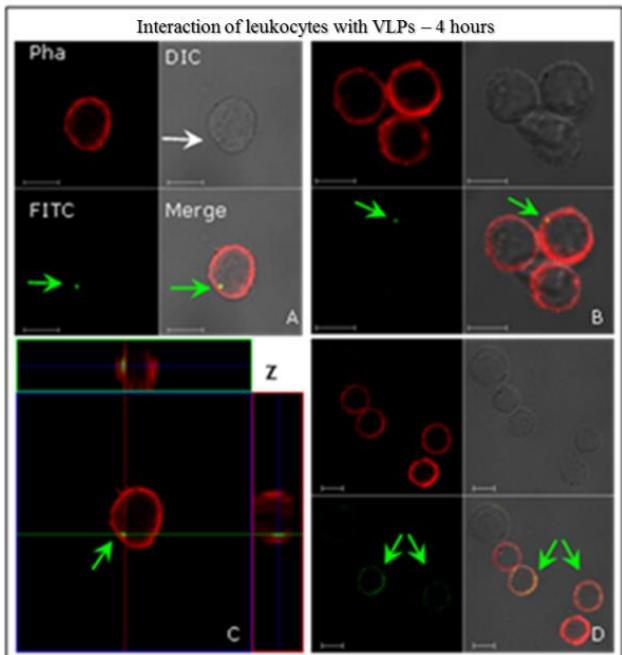
774 **Figure 1**

775
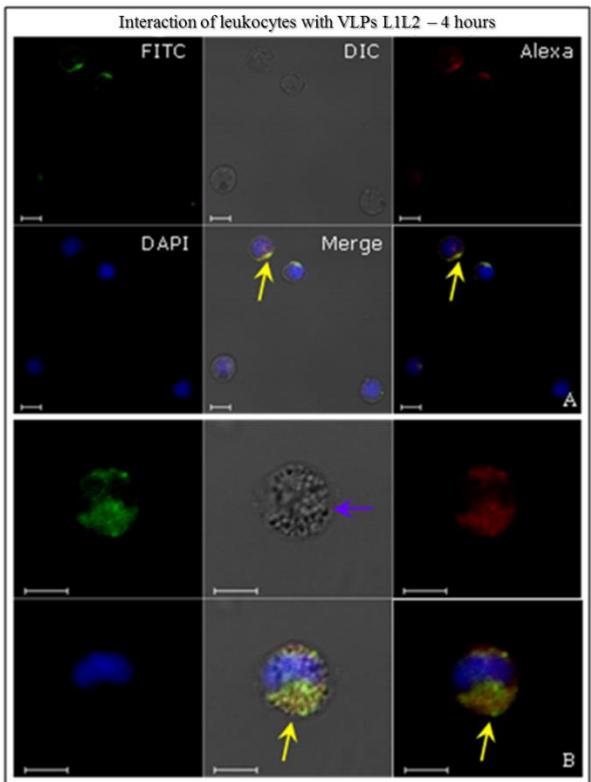
776

777 **Figure 2**
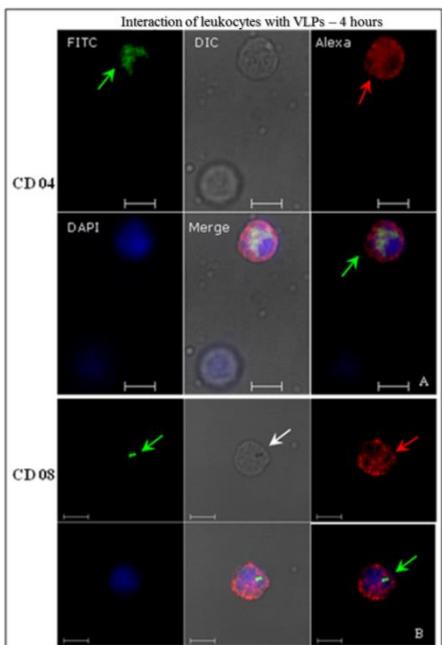
778

779 **Figure 3**
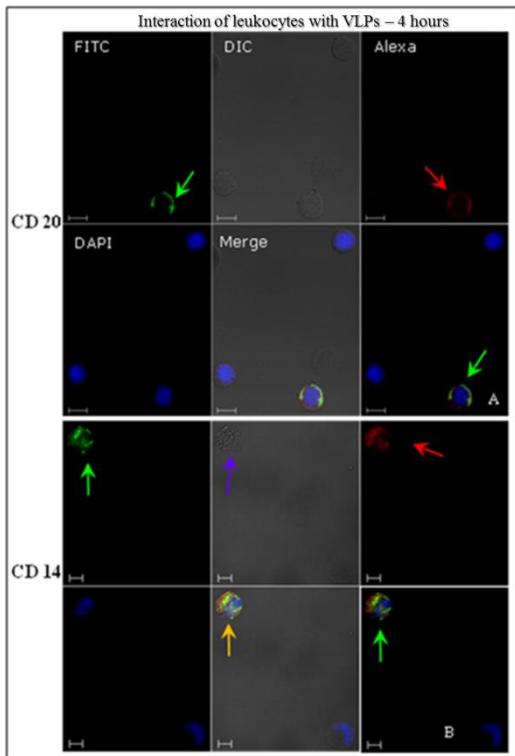
780

781 **Figure 4**
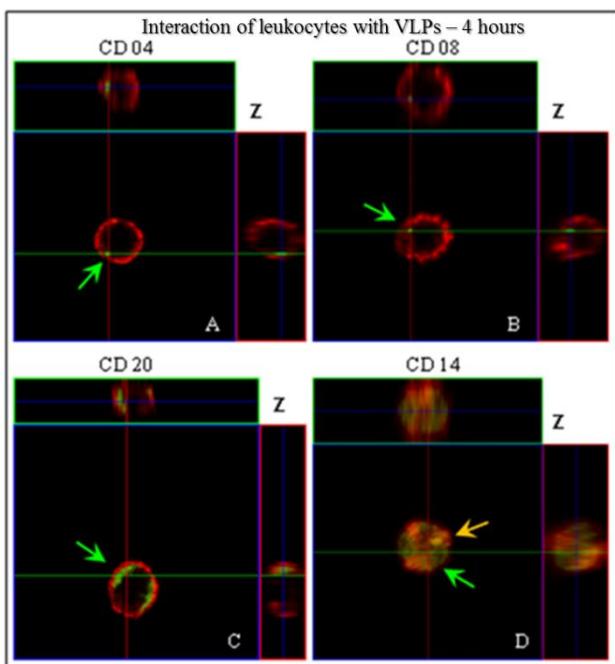
782

783   **Figure 5**
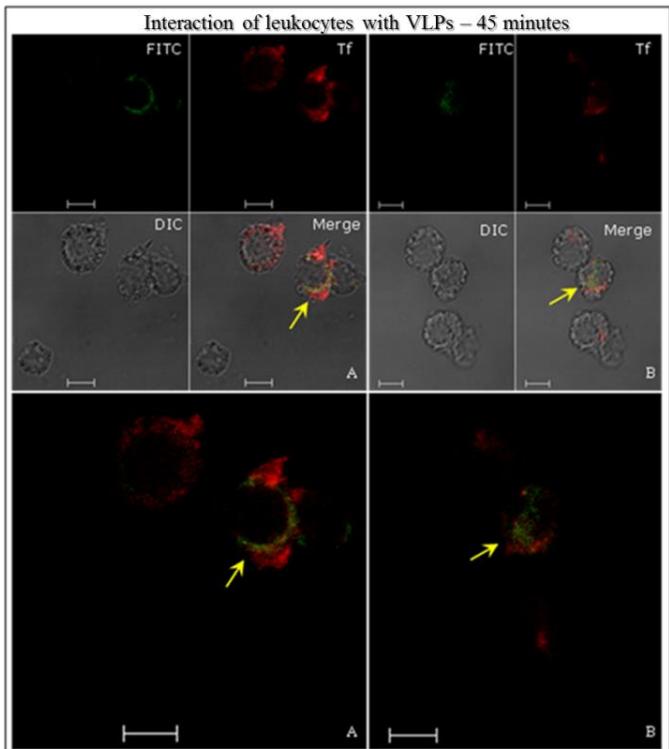
784

785   **Figure 6**
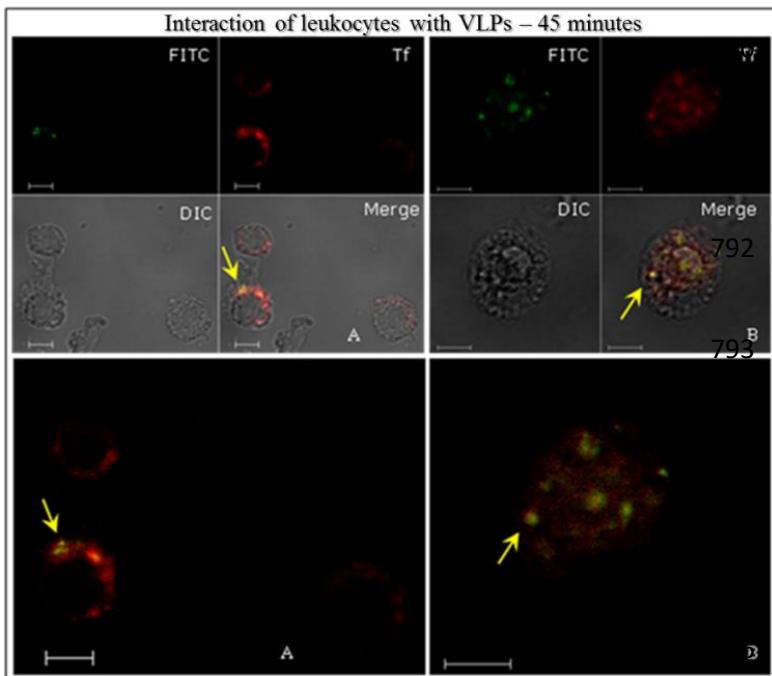
786

787 **Figure 7**
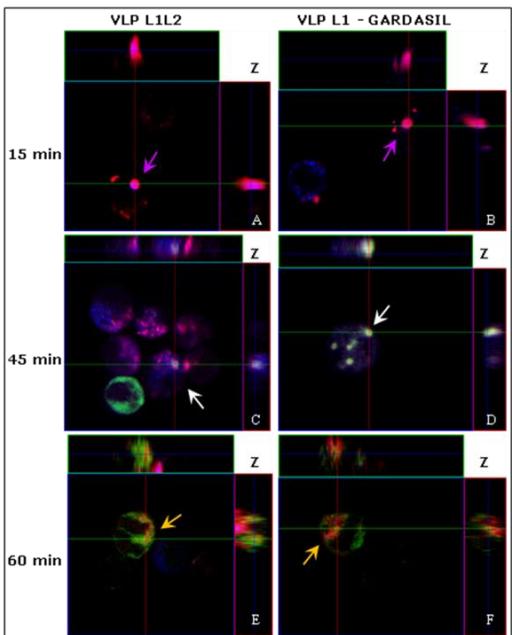
788

789 **Figure 8**
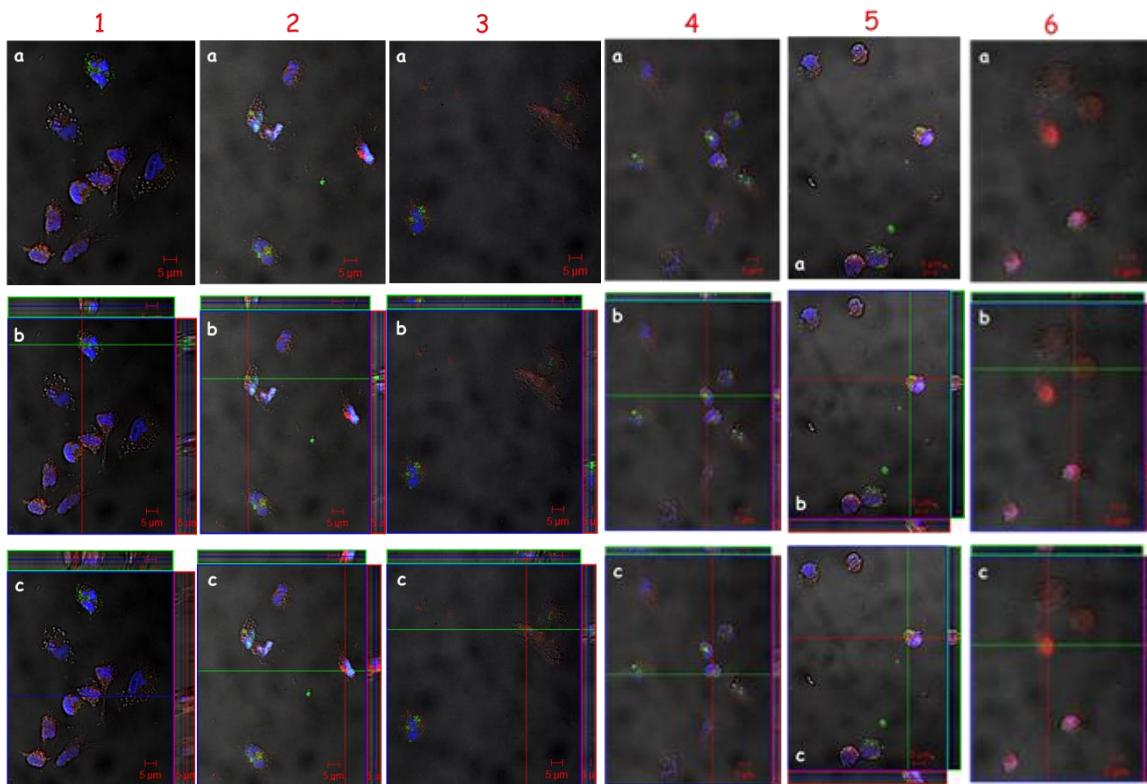
797   **Figure 9**
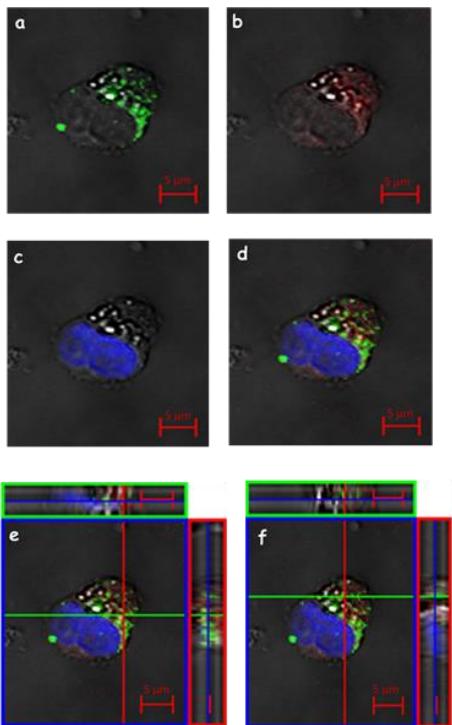
798

799   **Figure 10**

800

38

801 **Figure 11**

802

803

804

805

806

807

808

809

810

811

812

813

814

815

816

39
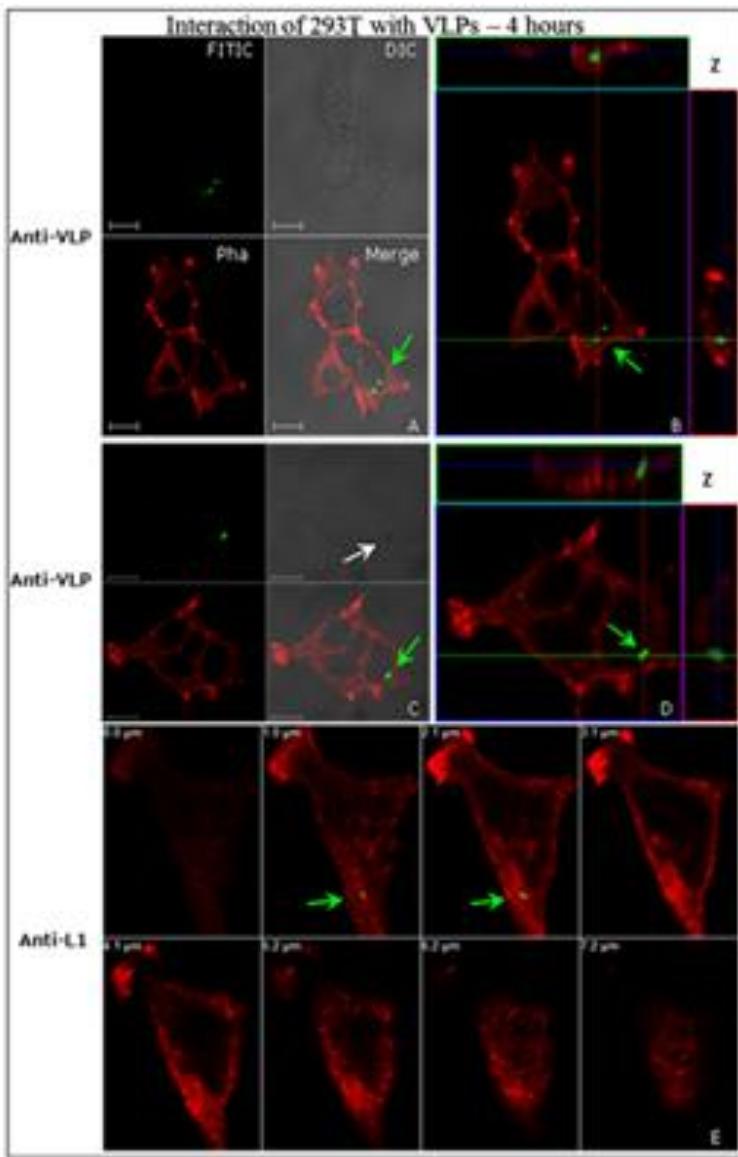
817 **Supplemental Material (Figures S1-S5 and Illustrations S6-S7)**

818 **Image 1 – S1**
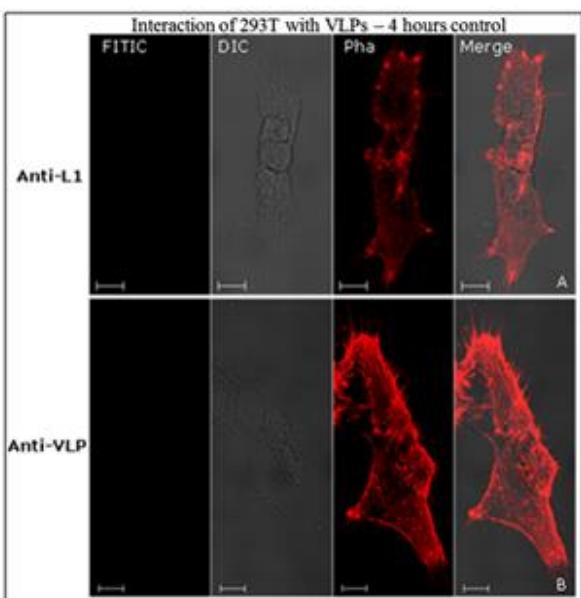
819

820 **Image 1 – S1:** Interaction of non-transfected HEK293T cell line with VLPs of HPV16,

821 detected by indirect immunofluorescence. Cells were incubated with the VLPs for 4 h,

822 fixed with 2% PFA in PBS. In (E) cells were immunostained with anti-L1 antibody and in

823 (A), (B), (C) and (D) anti-VLP conformational antibody, for both HPV16 and developed

824 with secondary antibody conjugated to FITC (green). Phalloidin detected the actin

825 cytoskeleton with AlexaFluor 594 conjugate (red). The internalisation of VLPs (green

826 arrows) are shown in B and D images, and L1 in E, sweep cuts through the Z axis (B) of

827 11.38 μm thick sections, and each section with 1.03 μm; (D) 9.67 μm thick sections and

828 each section having 1.61 μm. In (C), there was a similar structure to an endocytic vesicle

829 (white arrow). CLSM Zeiss LSM 510 Meta. Magnification: Objective C-Apochromatic

830 63xs /1.4 oil. Bar = 10 μm.

831
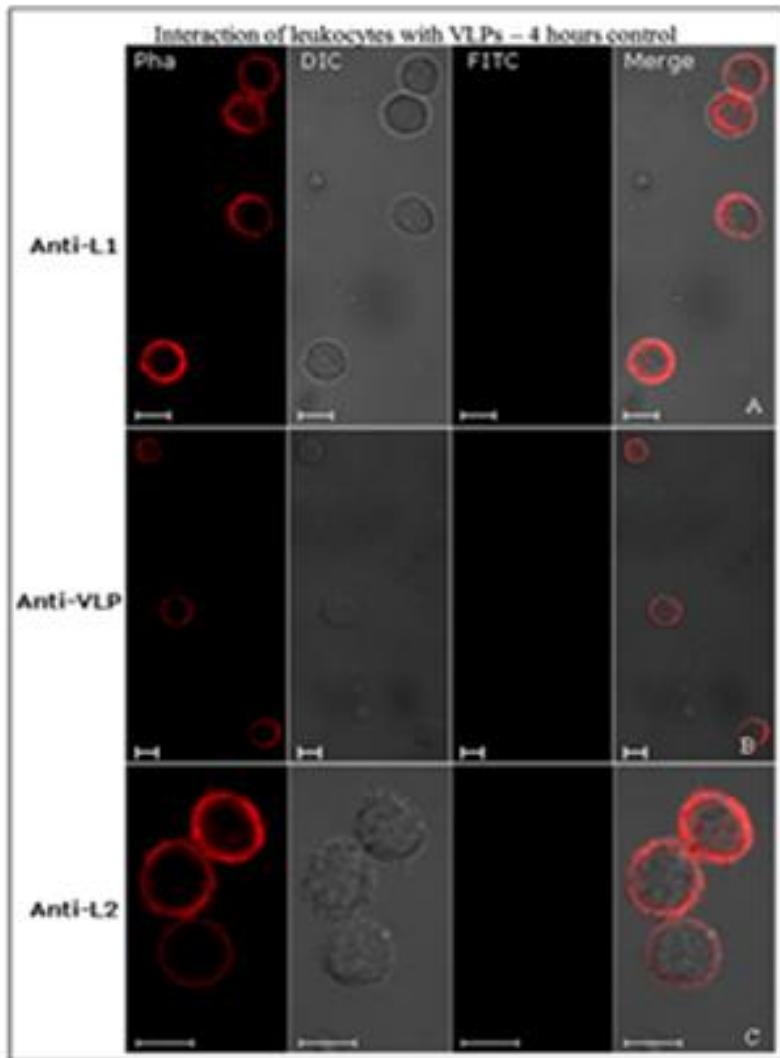
832 **Image 2 – S2**

833
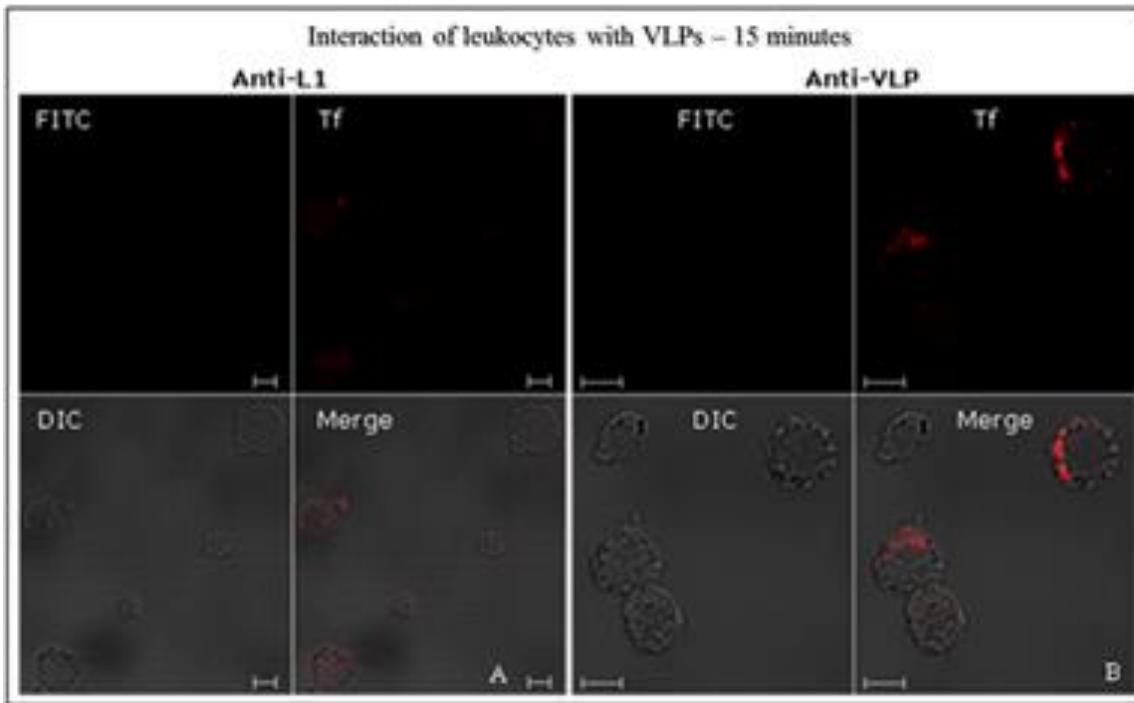
834 **Image 2 S2:** Assays-control of the interactions among HEK293T cells non-transfected,

835 with the HPV16 VLPs detected by immunofluorescence. In (A) cells were treated with anti-

836 L1 antibody and (B) with anti-VLP conformational, for both HPV16 and developed with

837 secondary antibody conjugated to FITC (green). AlexaFluor® 594-conjugated Phalloidin

838 (red) detected the actin cytoskeleton. CLSM Zeiss LSM 510 Meta. Magnification:

839 Objective C-Apochromatic 63xs /1.4 oil. Bar =10 μm.

840   **Image 3 – S3**

841

842   **Image 3 – S3:** Testing control the interactions of human leukocytes with VLPs of HPV16,

843   detected by indirect immunofluorescence. In (A) the cells were treated with anti-L1 and (B)

844   with anti-VLPs, HPV16 both to, and after, revealed by a secondary antibody conjugated to

845   FITC (green). In (C) the cells were treated with anti-HPV16 L2, and after, AlexaFluor®488

846   revealed by secondary antibody (green). AlexaFluor® 594-conjugated Phalloidin (red)

847   detected the actin cytoskeleton. CLSM Zeiss LSM 510 Meta. Magnification: Objective C-

848   Apochromatic 63xs /1.4 oil. Bar = 5 μm.

42

849 **Image 4 – S4**

850

851 **Image 4 S4:** Detection of HPV16 VLPs and Tf human leukocytes by indirect

852 immunofluorescence. The leukocyte cells were incubated with the VLPs and Tf protein

853 conjugated TexasRed® (red). In (A) the cells were immunostained with anti-L1 antibody

854 and (B) with anti-VLP conformational both to HPV16, revealed by a secondary antibody

855 conjugated to FITC (green). By confocality (merge) of the images is not possible to observe

856 colocalization and VLPs entry in leukocytes. CLSM Zeiss LSM 510 Meta. Magnification:

857 Objective C-Apochromatic 63xs /1.4 oil. Bar = 5 μm.

858
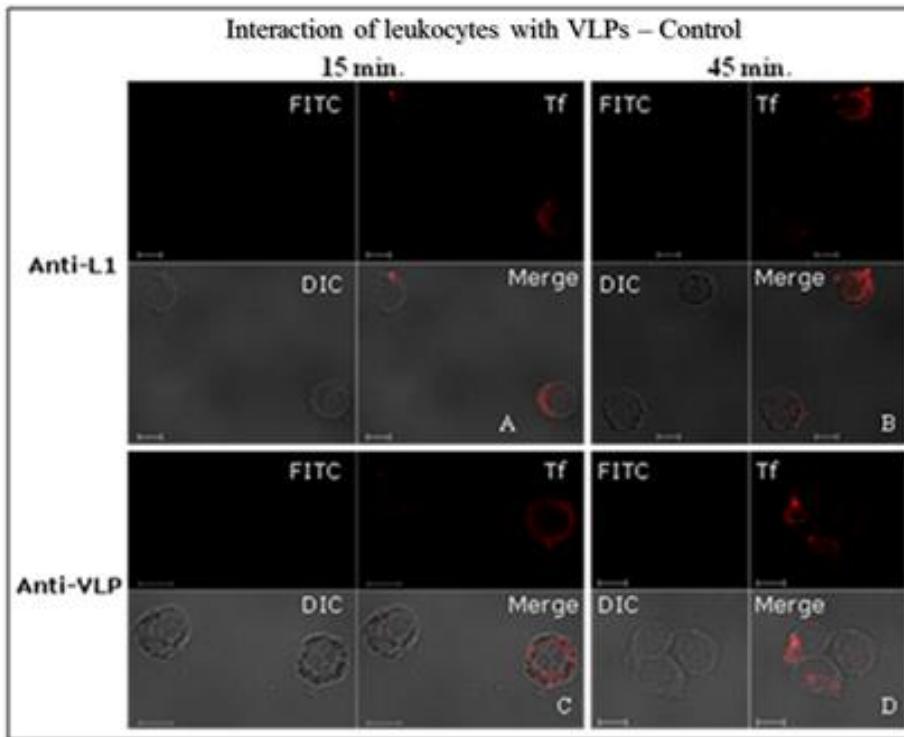
859

860

861

862

863 **Image 5 – S5**

864

865 **Image 5 - S5:** Images of the negative control testing of VLPs of HPV16 and Tf interactions

866 in human leukocytes analysed by indirect immunofluorescence. The leukocyte cells were

867 incubated with Tf conjugated TexasRed® (red) VLPs in the absence (A and C) and / or

868 denatured VLPs (B and D). In (A) and (C) the leukocytes were treated with anti-L1

869 antibody and (B) and (D) anti-VLPs, HPV16 both revealed by a secondary antibody

870 conjugated to FITC (green). Overlay (merge) of images that show no immunostaining signs

871 by anti-L1 and anti-HPV16 VLPs. CLSM Zeiss LSM 510 Meta. Magnification: Objective

872 C-Apochromatic 63xs /1.4 oil. Bar = 5 μm.

873

874

875

876

877 **Illustrations S6 – S7**

878 **S6 - Table 1:** List of primary antibodies used in immunocytochemistry reactions.

Antibody	Dilution	Description	Supplier
Anti-L1 Camvir-1	1:500	anti-mouse IgG$_{2a}$, specific for HPV16	BD Biosciences
Anti-L1 conformational	1:100	anti-mouse IgG$_{2a}$, specific for HPV16	Biodesign
Anti-L2	1:100	anti-rabbit IgG	Roden, R. MD/USA
Transferrin conjugated	1:60	TexasRed® (Ex. 595 nm, Em. 615 nm)	Molecular Probes™
Anti-Tf	1:750	anti- rabbit IgG	Dako
Anti-Ferritin	1:750	anti- rabbit IgG	Dako
Anti-CD71	1:750	anti-mouse IgG$_1$; Tf receptor	Dako
Anti-CD04	1:20	anti-mouse IgG$_{2a}$; recognizes T lymphocytes "helper"	CALTAG™ Laboratories
Anti-CD08	1:20	anti-mouse IgG$_{2a}$; recognizes cytotoxic T lymphocytes	CALTAG™ Laboratories
Anti-CD14	1:20	anti-mouse IgG$_{2a}$; recognizes monocytes	CALTAG™ Laboratories
Anti-CD20	1:20	anti-mouse IgG$_3$; recognizes B lymphocytes	CALTAG™ Laboratories

879

880 **S7 - Table 2:** List of secondary antibodies used in immunocytochemistry reactions.

Antibody	Dilution	Description	Ex/Em. (nm)	Supplier
FITC	1:250	anti- mouse IgG$_{2a}$	495/519	BD Biosciences
AlexaFluor®546	1:500	anti- mouse IgG	556/573	Molecular Probes™
AlexaFluor®555	1:500	anti- rabbit IgG	555/565	Molecular Probes™
AlexaFluor®594	1:500	anti- mouse IgG$_3$	590/617	Molecular Probes™
AlexaFluor®633	1:500	anti- mouse IgG	632/647	Molecular Probes™
AlexaFluor®633	1:500	anti- rabbit IgG	632/647	Molecular Probes™

881

45